

## Supporting Information

for

### **Interferometric Optical Sensors Based on Porous Silicon Grafted with Styrenic Moieties for Highly Enhanced VOC Detection**

Van-The Vo<sup>a</sup>, Abhijit. N. Kadam<sup>b</sup>, Thuy-An Nguyen<sup>\*c,d</sup>, and Sang-Wha Lee<sup>\*e</sup>

*<sup>a</sup>Long Son Petrochemicals Co., Ltd, Central Laboratory Department, Ho Chi Minh City, Vietnam*

*<sup>b</sup>Department of Chemistry, Wilson College (Autonomous), Mumbai 07, India*

*<sup>c</sup>Institute of Fundamental and Applied Sciences, Duy Tan University, Ho Chi Minh City 70000, Vietnam*

*<sup>d</sup>Faculty of Environmental and Chemical Engineering, Duy Tan University, Da Nang 50000, Vietnam*

*<sup>e</sup>Department of Chemical and Biological Engineering, Gachon University, South Korea*

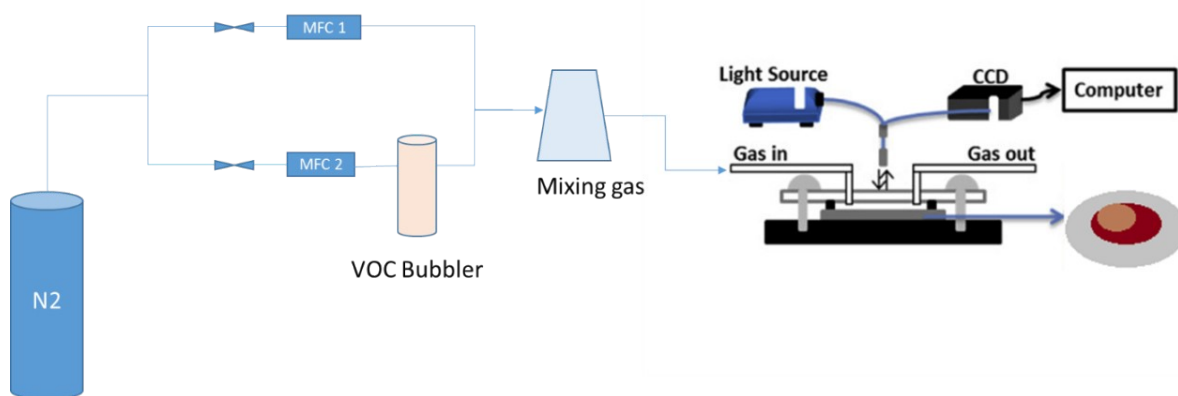
*\* E-mail: [nguyenthuyan3@duytan.edu.vn](mailto:nguyenthuyan3@duytan.edu.vn) (T.-A. Nguyen); [lswha@gachon.ac.kr](mailto:lswha@gachon.ac.kr) (S.-W. Lee)*

## S1. Instrumental analysis

Reflectance spectra were acquired using a CCD spectrometer (Ocean Optics USB-4000) fitted to a bifurcated fiber optic cable as described in [Figure S1](#). One arm of the fiber cable was connected to the spectrometer, while the other arm was connected to a tungsten light source (Ocean Optics LS-1). The distal end of the combined fiber was attached to a microscope objective lens to allow acquisition of 180° reflectance spectra from the sample surface, with a spot size of approximately 1–2 mm<sup>2</sup>. The porosity of pSi chips was characterized using the spectroscopic liquid infiltration method (SLIM). Fourier-transform infrared (FTIR) spectra were obtained using a Nicolet 6700 spectrometer (Thermo Scientific) equipped with an attenuated total reflectance (ATR) attachment. The ATR-FTIR spectral resolution was 4 cm<sup>-1</sup> and 128 scans were averaged per spectrum. Water contact angle measurements (Theta Optical Tensiometer, KSV, Finland) on the pSi chips were performed according to standard procedure. Plan-view and cross-sectional scanning electron microscope (SEM) were obtained using a field emission instrument (FEI XL30) operating at an accelerating voltage of 15 kV. Energy dispersive X-ray (EDX) spectroscopy was performed on cross-sectional samples using an accelerating voltage of 20 kV and a spot size of 4 μm.

## S2. RIFTS method

Reflective interferometric Fourier transform spectroscopy (RIFTS) was used to optically monitor the diffusion-controlled adsorption of analytes in the pSi chip. The focal point of RIFTS was approximately 1 mm in diameter, and this spot was positioned at the center of the pSi chip. The interference spectrum is originated from thin film Fabry–Pérot interference of light reflected from the air/porous Si and porous Si/crystalline Si interfaces. The interference spectrum is de-convoluted by applying a fast Fourier transform (FFT) to the reflectance vs frequency spectrum, which yields the value of the effective optical thickness,  $2nL$ , where  $n$  is the average refractive index of the porous layer and  $L$  is the thickness of the porous film. The quantity  $2nL$  is expected to increase with increasing the adsorbed amounts of analyte in the porous layer.



**Scheme S1.** Schematic set up of VOCs detection system.

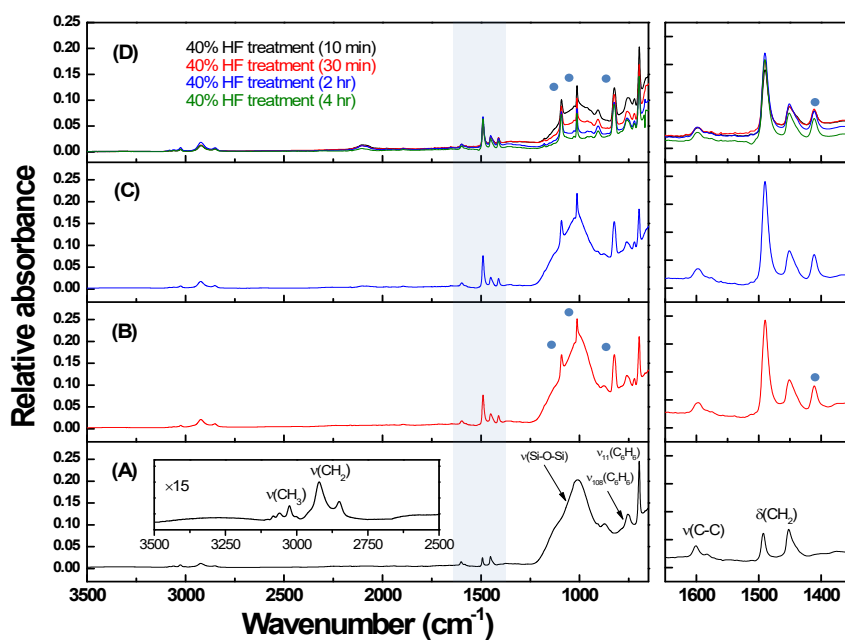


**Fig. S1.** FTIR spectra of the pSi samples at selected stages of preparation: **(A)** the pSi-PS composite after thermolysis of PS-loaded pSi, and soaking in toluene for 2 h to remove excess unreacted polymer; **(B)** the pSi-PS-PPCS composite after thermolysis of PPCS-loaded pSi-PS composite, and soaking in toluene for 2 h to remove excess unreacted polymer; **(C)** the pSi-PS-PPCS composite after treatment with 0.8% HF(aq) in 10% ethanol (15 min) to remove adventitious silicon oxide; **(D)** the pSi-PS-PPCS composite after treatment with 40% HF(aq) in 10% ethanol (from 10 min to 4 h) to remove adventitious silicon oxide

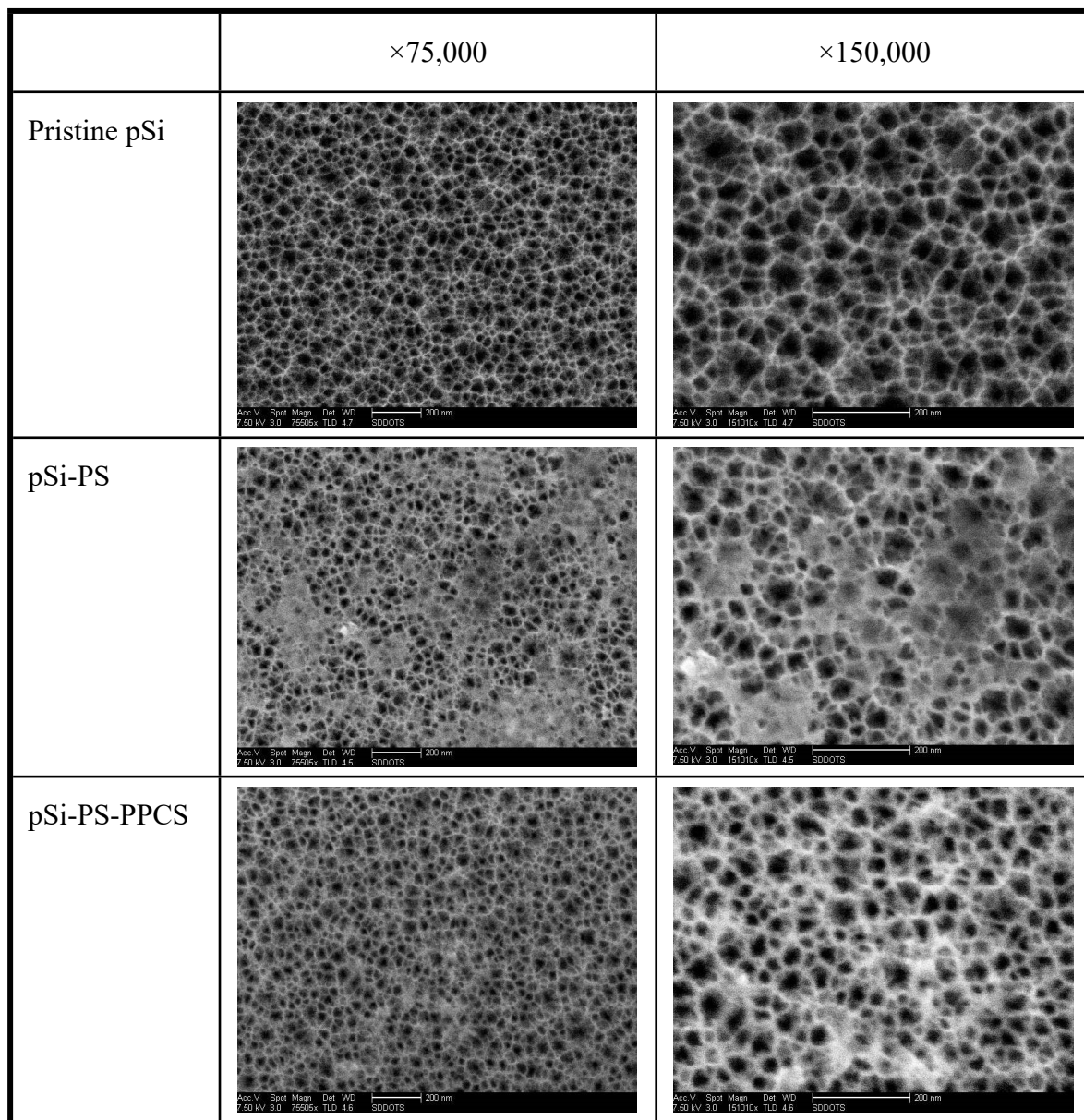


**Fig. S2.** SEM image of pSi, pSi-PS and pSi-PS-PPCS composite at different magnifications.

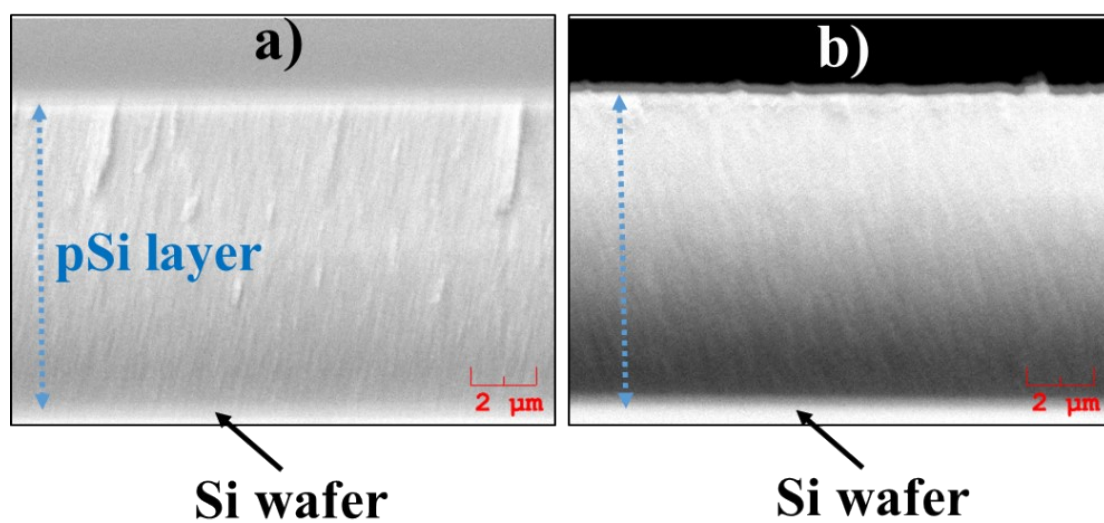


**Fig. S3.** Cross-sectional SEM images of a) pSi, b) pSi-PS-PPCS.

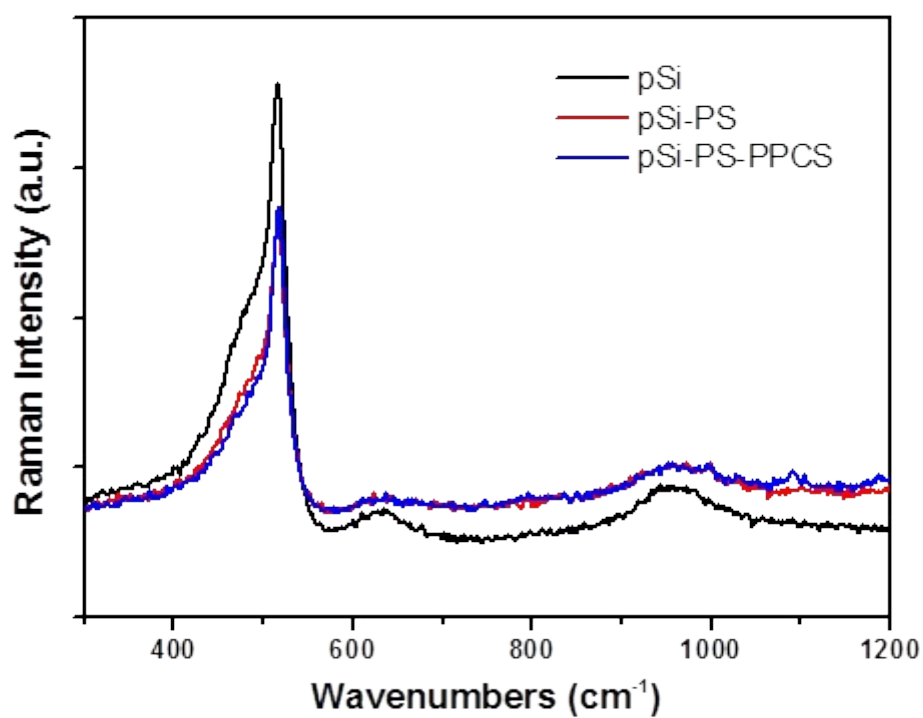


**Fig. S4.** Raman spectra of Oxidized pSi, pSi composites and PPCS-PS composite.

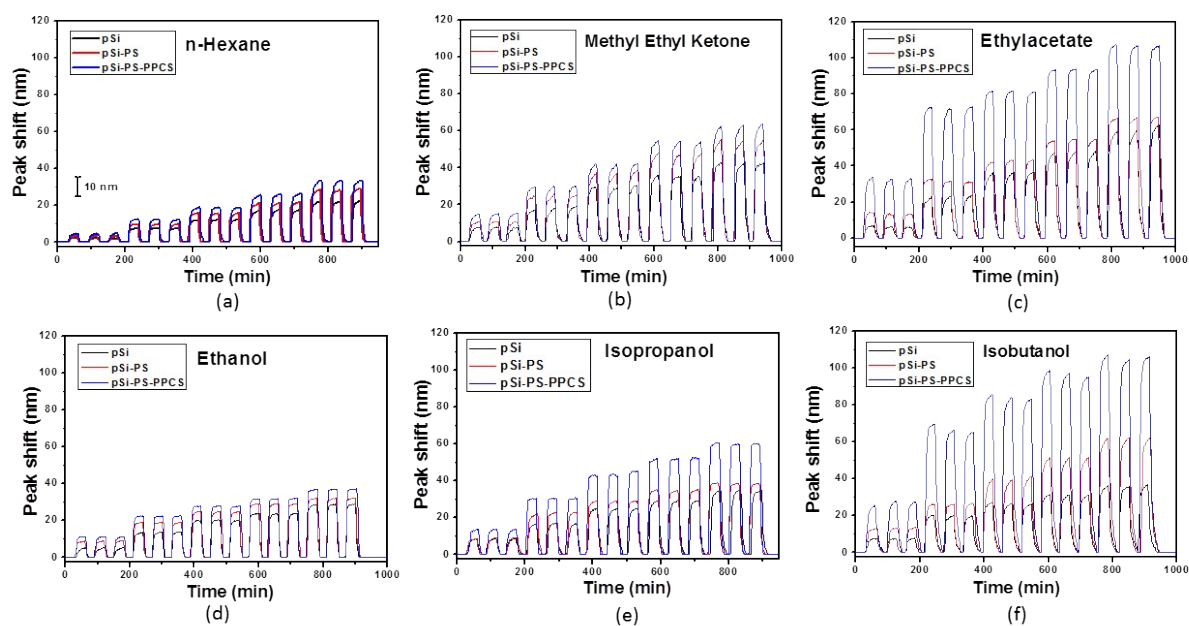


**Fig. S5.** Peak shift spectra of pristine pSi, pSi-PS, and pSi-PS-PPCS corresponding to the alternative flow (VOC flow/N<sub>2</sub> purging) of different VOCs: (a) hexane, (b) methyl ethyl ketone, (c) ethyl acetate, (d) ethanol, (e) isopropanol, (f) isobutanol.

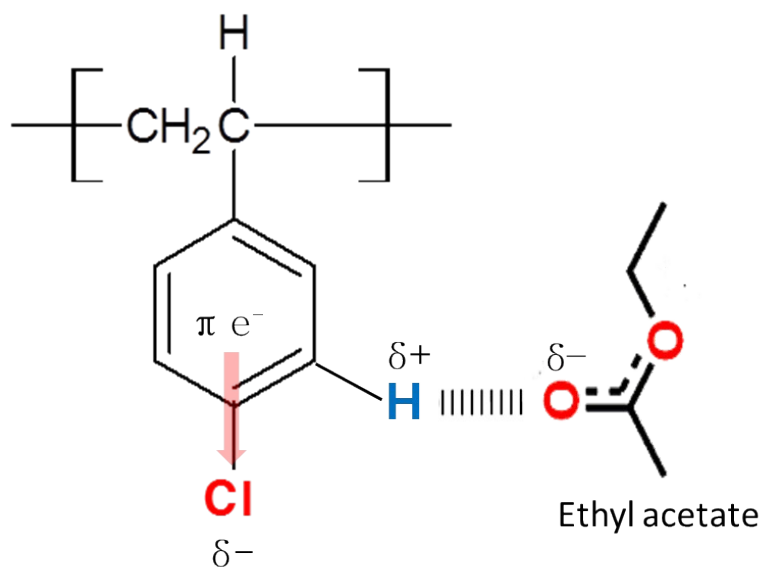


**Fig. S6.** Plausible hydrogen-bonding interaction mechanism between chlorine-substituted phenyl ring and resonant ethyl acetate.

**Table S1.** Comparison sensor performance for ethanol between pSi-PS-PPCS chip with other sensor materials.

Material	EtOH	Peak shift (nm)	Limit of Detection	Reference
Freestanding Parylene C and PMMA membrane on Si substrate	2.5 vol%	38.8	--	<sup>1</sup>
Nematic liquid crystal (NLC) film	--	--	247.42 ppm	<sup>2</sup>
Oxidized pSi rugate filter	0.05 P/P <sub>o</sub>	~7	--	<sup>3</sup>
Carbonized pSi rugate filter	0.05 P/P <sub>o</sub>	~5	--	<sup>3</sup>
PDMS coated micro-nano fiber	140 ppm	10.978		<sup>4</sup>
AgNP-decorated fabric	30-180 ppm	--	30 ppm	<sup>5</sup>
pSi-PS-PPCS	0.1 (vol%)	11.23	--	<i>This work</i>
	1.7 (vol%)	37.1	--	

## References

- 1 R. Sogame, Y. J. Choi, T. Noda, K. Sawada and K. Takahashi, *Sensors*, 2024, **24**.
- 2 M. Gu, H. Chen and L. Li, *Sensors and Actuators A: Physical*, 2025, **387**, 116481.
- 3 J. D. Kittle, J. S. Gofus, 3rd, A. N. Abel and B. D. Evans, *ACS omega*, 2020, **5**, 19820-19826.
- 4 B. Shi, Y. Sun, W. Zheng, N. Zhu and Y.-n. Zhang, 2020, DOI: 10.1109/ccdc49329.2020.9164346, 4959-4962.
- 5 S. J. Shaikh, A. J. Rodge, A. M. N. S. Siddiqui, A. B. U. Rahman, P. M. Khanzode, K. A. Bogle, V. N. Narwade, S. S. Dahiwalé and M. S. Sahasrabudhe, *Advanced Engineering Materials*, 2025, **27**.